MR signal-fat-fraction analysis and T2*weighted imaging measure BAT reliably on humans without cold exposure

Holstila, Milja; Pesola, Marko; Saari, Teemu; Koskensalo, Kalle; Raiko, Juho; Borra, Ronald J. H.; Nuutila, Pirjo; Parkkola, Riitta; Virtanen, Kirsi A.

Published in:
Metabolism

DOI:
10.1016/j.metabol.2017.02.001

Publication date:
2017

Available online at www.sciencedirect.com

Metabolism

www.metabolismjournal.com

Methods

MR signal-fat-fraction analysis and T2* weighted imaging measure BAT reliably on humans without cold exposure

Milja Holstila[a,b,c,*], *Marko Pesola*[d], *Teemu Saari*[b], *Kalle Koskensalo*[a], *Juho Raiko*[a,b], *Ronald J.H. Borra*[c,e], *Pirjo Nuutila*[a,b], *Riitta Parkkola*[b,c], *Kirsi A. Virtanen*[a,b]

[a] *Turku PET Centre, Turku University Hospital, Turku, Finland*
[b] *Turku PET Centre, University of Turku, Turku, Finland*
[c] *Medical Imaging Centre of Southwest Finland, Turku University Hospital, Turku, Finland*
[d] *Medical Imaging and Radiation Therapy, Carea, Kymenlaakso Social and Health Services, Kotka, Finland*
[e] *Department of Nuclear Medicine and Molecular Imaging, University of Groningen, University Medical Center Groningen, Groningen, Netherlands*

ARTICLE INFO

Article history:
Received 25 September 2016
Accepted 1 February 2017

Keywords:
Brown adipose tissue
Triglyceride content
Magnetic resonance imaging
^{18}F-FDG positron emission tomography
Obesity

ABSTRACT

Objective. Brown adipose tissue (BAT) is compositionally distinct from white adipose tissue (WAT) in terms of triglyceride and water content. In adult humans, the most significant BAT depot is localized in the supraclavicular area. Our aim is to differentiate brown adipose tissue from white adipose tissue using fat T2* relaxation time mapping and signal-fat-fraction (SFF) analysis based on a commercially available modified 2-point-Dixon (mDixon) water–fat separation method. We hypothesize that magnetic resonance (MR) imaging can reliably measure BAT regardless of the cold-induced metabolic activation, with BAT having a significantly higher water and iron content compared to WAT.

Material and methods. The supraclavicular area of 13 volunteers was studied on 3 T PET–MRI scanner using T2* relaxation time and SFF mapping both during cold exposure and at ambient temperature; and ^{18}F-FDG PET during cold exposure. Volumes of interest (VOIs) were defined semiautomatically in the supraclavicular fat depot, subcutaneous WAT and muscle.

Results. The supraclavicular fat depot (assumed to contain BAT) had a significantly lower SFF and fat T2* relaxation time compared to subcutaneous WAT. Cold exposure did not significantly affect MR-based measurements. SFF and T2* values measured during cold exposure and at ambient temperature correlated inversely with the glucose uptake measured by ^{18}F-FDG PET.

Conclusions. Human BAT can be reliably and safely assessed using MRI without cold activation and PET-related radiation exposure.

Abbreviations: BAT, Brown adipose tissue; BOLD, Blood-oxygen-level dependent; ^{18}F-FDG, ^{18}F-fluorodeoxyglucose; FFE, Fast field echo; fMRI, Functional magnetic resonance imaging; GRE, Gradient echo; ^{1}H MRS, Single-voxel proton magnetic resonance spectroscopy; MR, Magnetic resonance; MRI, Magnetic resonance imaging; PET, Positron emission tomography; SFF, Signal-fat-fraction; SPIR, Spectral presaturation with inversion recovery; T1w, T1-weighted; T2w, T2-weighted; T2*w, T2*-weighted; TE, Echo time; TR, Time of repetition; VOI, Volume of interest; WAT, White adipose tissue.

* *Corresponding author at:* Department of Radiology, Turku University Hospital, P.O. Box 52, FI-20521 Turku, Finland. Tel.: +358 2 313 2982; fax: +358 2 313 2950.
E-mail address: milja.holstila@utu.fi (M. Holstila).

http://dx.doi.org/10.1016/j.metabol.2017.02.001
0026-0495/

1. Introduction

1.1. Background

Brown adipose tissue (BAT) is fat tissue characterized by a higher water and lower triglyceride content, as well as higher number of intracellular lipid droplets and mitochondria relative to white adipose tissue (WAT) [1]. BAT may be activated for instance by cold exposure to generate heat [2,3]. BAT is prevalent in newborns and in childhood with increasing activity until adolescence [4], but prevalence gradually decreases with age [5]. There are two different types of BAT in humans: infants have "classic BAT" in the interscapular area, while adults seem to have "inducible thermogenic BAT", which is also known as beige or brite fat derived from the same adipogenic lineage as white adipocytes [6,7]. The cells can take on the appearance and function of BAT upon prolonged stimulation by cold, but the process can also be reversed. Thus adult human BAT contains a mixture of brown and white adipocytes at different stages [8], and as a result the tissue triglyceride content is a continuous spectrum. These properties make accurate definition and differentiation of BAT from surrounding tissue very challenging.

The most prominent BAT depot in adult humans is localized in the supraclavicular area [9,10]. Decreases in BAT mass and activity may have a role in the development of obesity and diabetes in adulthood. Human BAT is highly insulin-sensitive [11] and BAT metabolic activity measured by ^{18}F-FDG PET correlates positively with whole-body insulin sensitivity [12] and inversely with total body fat [3].

The in vivo localization and activation state of BAT can be assessed by ^{18}F-fluorodeoxyglucose (^{18}F-FDG), a radiolabeled analog of glucose used as a tracer in positron emission tomography (PET) [13,14]. Although considered a noninvasive method, ^{18}F-FDG-PET/CT imaging involves intravenous injection of radioactive tracer, as well as additional radiation exposure due to CT. Furthermore the cooling procedure needed to metabolically activate BAT for ^{18}F-FDG-PET examination is lengthy and uncomfortable. ^{18}F-FDG-PET has the specific ability to quantify metabolic activity in BAT, while MR imaging can reliably measure BAT regardless of the activation state, with BAT having a significantly higher water content compared to WAT [15]. MR imaging methods that have been used to examine BAT include water saturation efficiency measurement [16], blood-oxygen-level dependent (BOLD) functional MRI (fMRI) [17], SFF analysis of mDixon images [16–22], T2* relaxation time mapping [17,18,20] and single-voxel proton magnetic resonance spectroscopy (^{1}H MRS) [15,23].

MDixon is a commercially available method [24,25] that uses a gradient echo (GRE) pulse sequence to acquire a conventional field echo image with water and fat signals in different phases relative to another. A water-only image and a fat-only image can be generated from these images, and subsequently those can be used for constructing SFF maps, showing the fat/water percentage and allowing direct image based water and fat quantitation. Brown adipose cells contain more water and less lipids than white adipose cells, and BAT is also more vascular tissue than WAT. These contribute to the lower SFF in BAT compared to WAT [15].

T2* relaxation time represents the transverse magnetization decay, caused by a combination of spin–spin relaxation and local magnetic field inhomogeneity [26]. Brown adipocytes have more mitochondria than white adipocytes. Also, blood perfusion and oxygen consumption in BAT increase when the tissue is stimulated [27], and consequently BAT has higher levels of deoxyhemoglobin. Mitochondria and deoxyhemoglobin are both rich in iron, which contributes to the lower T2* relaxation time in BAT.

1.2. Rationale

In this study our objective is to study BAT using SFF and T2* relaxation time mapping during both cold exposure and at ambient conditions. The specific aims of this study are as follows: (1) measure BAT, WAT and muscle SFF and T2* values, (2) correlate SFF and T2* measurements with ^{18}F-FDG-PET, and (3) examine the effect of cold exposure on SFF and T2* measurements.

2. Methods

2.1. Ethical Approval

The study protocol was reviewed and approved by the ethics committee of the Hospital District of Southwest Finland. Study subjects were recruited with newspaper or electronic board advertisements, and each gave written informed consent prior to the examinations as recommended by the Declaration of Helsinki.

2.2. Study Design

Subjects were first interviewed and screened by a licensed physician to exclude subjects with diabetes. Subjects with normal glucose tolerance (serum fasting plasma glucose less than 5.6 mmol/l and a 2-h oral glucose tolerance test (OGTT) with 75 g glucose intake with plasma glucose less than 7.8 mmol/l) were included (n = 13). The age range was 19–55, mean age 32.7 ± 9.9 years. Nine of the subjects were of normal weight (BMI 20.3–24.7 kg/m^2), three were overweight (BMI 25.0–31.5 kg/m^2) and one was obese (BMI 31.5 kg/m^2). Both genders were studied (6 F/7 M).

The subjects were exposed to cold conditions prior to the first examination to metabolically activate BAT, as previously described [27]. Before being positioned in the scanner for the cold-exposure scan, the subject, while wearing light clothing, spent 120 min lying on a bed with a water circulated cooling blanket (Blanketrol III, Cincinnati Sub-Zero, Cincinnati, OH, USA) beneath the trunk and legs and a similar blanket on top of them. The temperature of the water inside the blanket was first set to +5 °C and then adjusted accordingly in order to achieve non-shivering thermogenesis by raising the temperature of the blankets in case of the subject shivering. During the 3 T PET–MR scan cold exposure was maintained by placing cold packs around the lower extremities of the subject. All scans were obtained in the morning, during the months from September to April. The mean time between the scans on each individual was 24 ± 27 days. The subjects were advised to fast overnight and to

avoid exercise for 24 h and ingesting alcohol or high-fat meals for 72 h prior to the examination. Room temperature was maintained at approximately 22 °C [27].

2.3. MRI and ^{18}F-FDG-PET Measurements

MRI scans were conducted both during cold exposure and at ambient room temperature conditions without specific preparations using a Philips Ingenuity 3 T PET–MR scanner (Philips Healthcare, Cleveland). The MR examination was performed using a two channel whole body RF coil for excitation while signal was measured using a 32 channel cardiac coil. Both MRI and PET measurements were performed in all subjects in the supraclavicular and neck area (Fig. 1).

The first imaging session started with cold exposure, followed by a dynamic ^{18}F-FDG-PET examination. Blood glucose was measured previous to the PET exam as well as every 60 min during the imaging. ^{18}F-FDG was synthesized in accordance with the standard manufacturing procedures of the Turku PET Centre. A batch of ^{18}FDG was only released for use if the standard operating procedure had been followed and the radiochemical purity exceeded 90%. An intravenous injection of ^{18}F-FDG (185 MBq) was given into the antecubital vein, and a dynamic scan with variable frame lengths (40 min; 4 × 30 s, 1 × 60 s, 1 × 120 s, 3 × 300 s, 2 × 600 s) of the neck and upper thoracic region was performed. After acquisition the resulting dynamic data were reconstructed. During this process the numerical PET data (i.e. number of counts per detection channel) were converted to PET images. All emission scans were reconstructed with iterative ML-OSEM reconstruction, resulting in a transaxial spatial resolution of about 5 mm in the field of view. The matrix included 128 × 128 pixels. The data from the transmission scans were used to correct the corresponding emission scans for photon attenuation. Furthermore, the PET data were corrected for decay, scattered radiation and random coincidences. The summation images of the dynamic PET images were made to obtain a better statistical reference for the co-registration with MRI images.

In the same session, using the same scanner, the following MRI sequences were performed: A modified 2-point Dixon sequence (mDixon) was used to provide anatomical reference

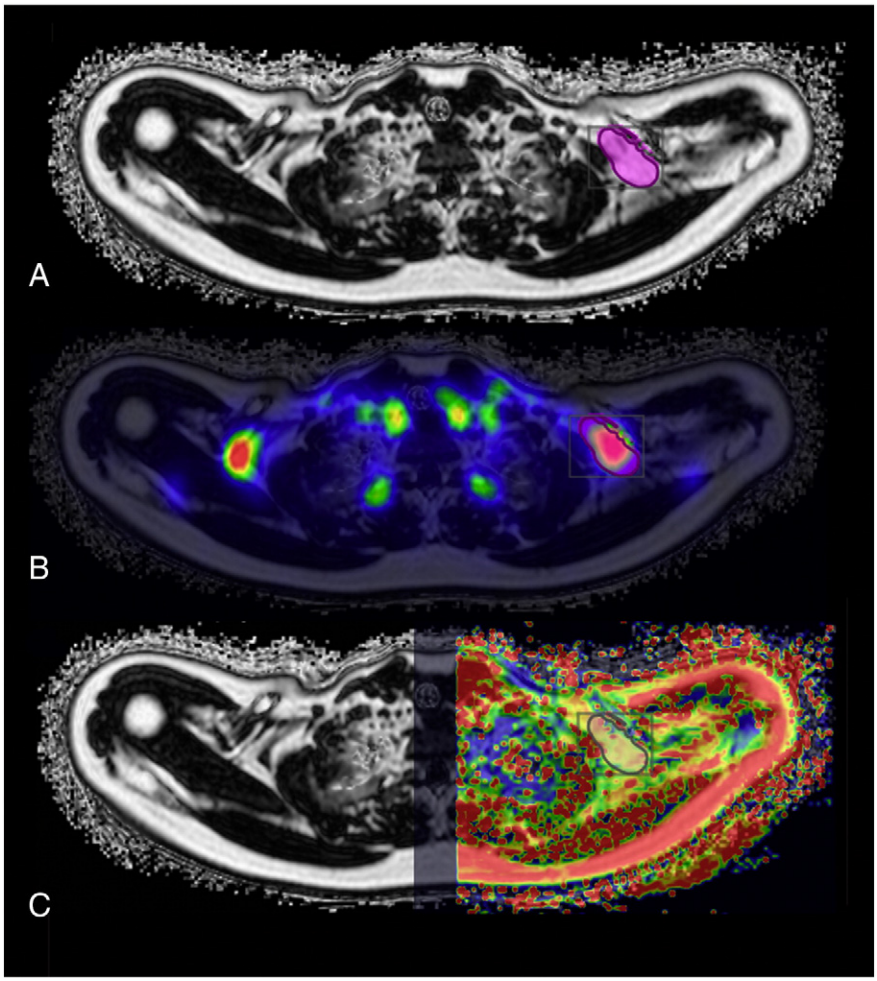

Fig. 1 – MR and ^{18}F-FDG PET imaging. VOI was drawn semiautomatically on left supraclavicular fat depot. All the MRI measurements and the glucose uptake measured on ^{18}F-FDG-PET were calculated using the same VOI. SFF map calculated from mDixon images (A). ^{18}F-FDG-PET glucose uptake image (B) and fat T2* relaxation time map of the left side (C) fused with the SFF map for anatomical reference.

in the neck and body area and for calculating SFF maps. The mDixon sequence was an FFE 3D based sequence with TE1 = 1.07 ms, TE2 = 1.9 ms and TR = 3.1 ms. Voxel size was 1.75 mm × 2 mm × 1.5 mm and 133 slices were collected with an acquisition time of 16 s. Scans were performed using axial, coronal and sagittal slice orientations. No breath-hold was used.

Fat and water suppressed multi-echo flyback FFE3D scans were performed to obtain T2* maps separately for water and fat. SPIR was used to suppress signal from either fat or water to obtain signal decay free of fat–water resonance frequency difference modulation. TR was 70 ms and the first TE 1.15 ms. Ten echoes with an echo spacing of 1.1 ms were collected. Flip angle was 20° and two averages were collected with voxel size 2 mm × 2 mm × 3 mm. Number of slices was 10 and SENSE factor 2 in anteroposterior direction. Total scan duration was 2 min 56 s. No breath-hold was used. The MRI scan obtained in warm conditions was performed on a separate day, with the use of the same MRI scanning protocol, except for no ^{18}F-FDG-PET examination or cold exposure before or during the procedure.

2.4. Image Post-Processing

T2* relaxation maps were calculated with OsiriX v.6.0.2 software (Pixmeo, Geneva, Switzerland). SFF was calculated from the ratio of fat signal to the summed water and fat signal and analyzed using commercial Philips software on the MR scanner console. The image series were visually examined by an experienced radiologist to ensure the quality of the data. Volumes of interest (VOIs) were drawn on semiautomatically including the whole anatomical supraclavicular fat depot using the Carimas 2.9 software package (Turku PET Centre, Turku, Finland). The volume of the VOI depended of the size of the subject and the relative size of the supraclavicular fat depot (mean 29.2 ± 9.2 cm^2 after cold exposure, 29.2 ± 10.6 cm^2 at ambient conditions). A rough 3D VOI was drawn on SFF images using the sphere tool of Carimas which was subsequently edited with the vertex function, taking great care to avoid the lungs, the subcutaneous fat and the bone marrow. After that, the ROI was automatically cropped using the histogram tool in Carimas, with the threshold of 50%–100% SFF. The resulting 3D VOI was reduced twice in size using the automatic shrink option, to avoid possible contamination of nearby tissues resulting from chemical shift artifacts or small motion artifacts. The 3D VOIs on subcutaneous WAT and infraspinatus muscle were drawn as ellipsoids using the Carimas sphere tool, assuring an appropriate margin in relation to other tissues. SFF data, ^{18}F-FDG uptake and T2* maps were co-registered and analyzed with the Carimas 2.9 software package using the VOIs described above.

2.5. Anthropometric Measurements

Waist circumference was measured at the navel level and hip circumference at the major trochanter level. Weight was determined using weighing scales (Seca, Hamburg, Germany) and height with measurement tape. Body mass index was calculated as the weight in kilos divided by the height in meters squared.

2.6. Statistical Analysis

Correlations were performed using Pearson's correlation with the T2* values, SFF values and ^{18}F-FDG uptake assumed to be continuous variables. Mixed model repeated measures analysis was performed to analyze the possible differences between the examinations acquired during cold exposure and at ambient conditions and to compare the different VOIs (BAT, WAT, muscle) to each other. P values <0.05 were considered significant. Statistical analyses were performed with SAS for Windows version 9.4 (SAS Institute, Cary, NC, USA).

3. Results

3.1. SFF Maps

SFF studies were performed during cold exposure and at ambient conditions. Regardless of cold exposure, measurements showed a supraclavicular BAT depot containing water and fat, with significantly lower SFF compared to subcutaneous WAT (mean 81.9 ± 4.0% in BAT vs 90.0 ± 2.9% in WAT, $p < 0.0001$ during cold exposure and 82.3 ± 3.8% in BAT vs 89.1 ± 3.2% in WAT, $p < 0.0001$, at ambient temperature) (Figs. 1 and 2). Thus, cold exposure did not significantly change BAT SFF ($p = 0.62$). Cold-induced glucose uptake measured with ^{18}F-FDG-PET correlated with BAT SFF measured both during cold exposure ($p = 0.02$, $r = -0.64$) and at ambient conditions ($p = 0.02$, $r = -0.63$). The areas with lower SFF (assumed to be BAT) in the supraclavicular fat depot could also be clearly detected visually. SFF of muscle was low both during cold exposure (mean 6.7 ± 1.4% vs mean 81.9 ± 4.0% in BAT, $p < 0.00000000001$) and at ambient conditions (7.6 ± 2.4% vs 82.3 ± 3.8% in BAT, $p < 0.00000000001$), and cold exposure had no significant effect on the values ($p = 0.40$). (Table 1 and 2).

3.2. T2* Relaxation Time Mapping

T2* mapping was performed during cold exposure and at ambient conditions. T2* of BAT differed significantly from that of WAT (15.3 ± 1.1 ms vs 20.7 ± 2.0 ms, $p = 0.0001$, during cold exposure, 14.8 ± 1.8 ms vs 20.4 ± 1.4 ms, $p = 0.0001$, at ambient conditions). Cold exposure did not have significant effect on BAT T2* relaxation times (15.3 ± 1.1 ms during cold exposure vs 14.8 ± 1.8 ms at ambient conditions, $p = 0.31$). T2* relaxation times measured during cold exposure and at ambient conditions both correlated significantly ($p = 0.001$, $r = -0.79$ and $p = 0.02$, $r = -0.65$, respectively) with BAT glucose uptake measured during cold exposure. BAT had markedly higher T2* time compared to muscle (15.3 ± 1.1 ms vs 28.6 ± 3.4 ms, $p < 0.0001$ during cold exposure, 14.8 ± 1.8 ms vs 25.6 ± 3.4 ms, $p < 0.0001$ at ambient conditions). (Table 1 and 2).

3.3. ^{18}F-FDG PET

During cold exposure, 12 of the 13 subjects exhibited supraclavicular BAT activation higher than WAT and adjacent muscle as measured with ^{18}F-FDG-PET. The most prominent glucose uptake in PET images was observed in the supraclavicular fat depot, in several cases continuing in the lateral cervical area.

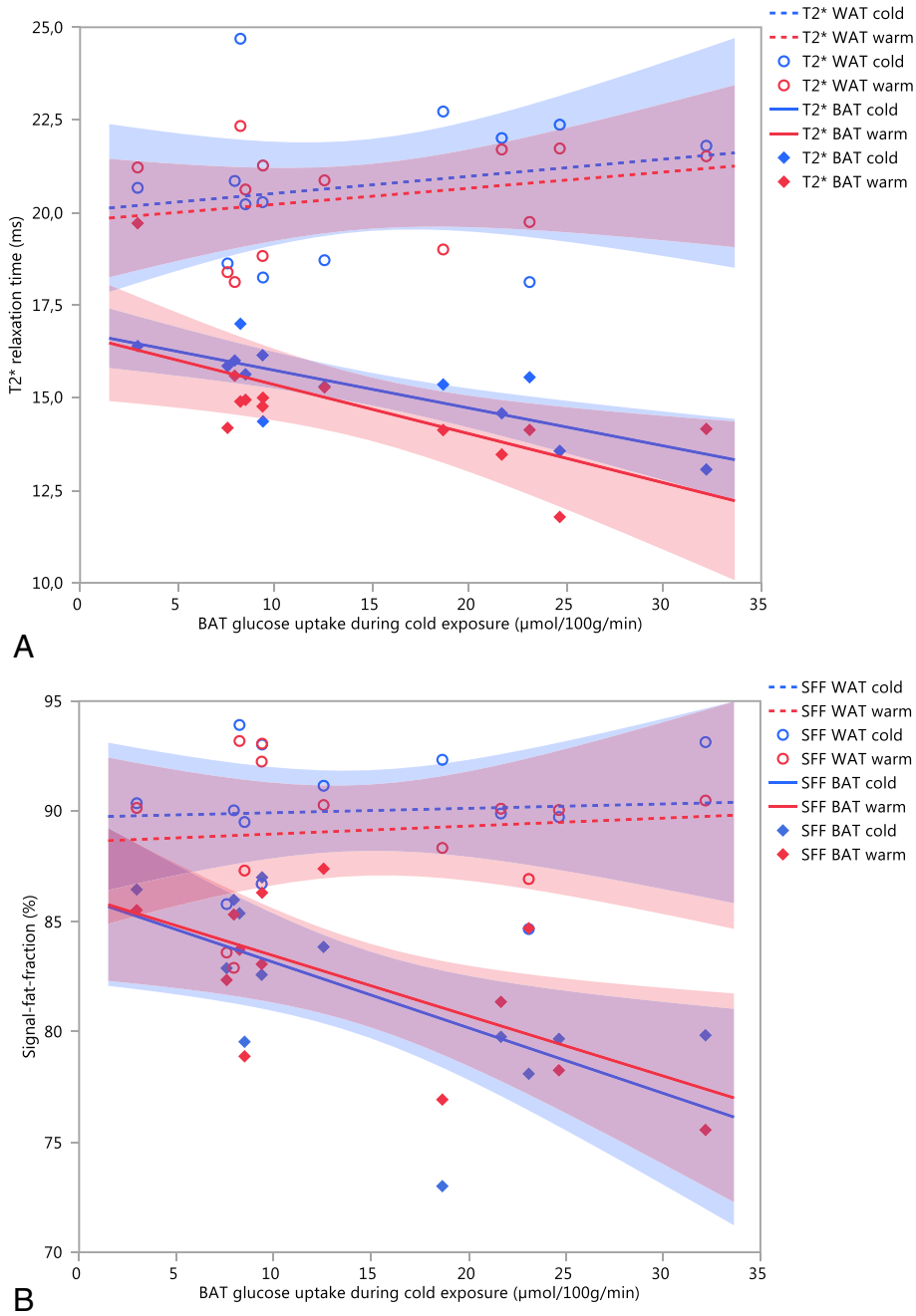

Fig. 2 – Cold exposure did not significantly affect MRI-based measurements. T2* (A) and SFF map (B) during cold exposure and at ambient conditions, shown as linear regression model with confidence intervals.

Supraclavicular (BAT) glucose uptake varied between 3.0 and 32.2 μmol/100 g/min, mean 14.4 ± 8.7 μmol/100 g/min, while WAT uptake varied between 1.1 and 3.4 μmol/100 g/min, mean 3.0 ± 0.3 μmol/100 g/min, and muscle uptake between 1.5 and 3.6 μmol/100 g/min, mean 2.7 ± 0.7 μmol/100 g/min. BAT activity on ^{18}F-FDG PET did not correlate with age (r = −0.31) or BMI (r = 0,11). (Table 1, Table 2)

3.4. *The Subject Who did not Exhibit BAT*

The one subject lacking BAT activation was 45 years old, the 2nd oldest in this group. He was of normal weight (BMI 22.4 kg/m^2), and his blood glucose level was normal, with baseline 5.55 mmol/l and 2 h OGTT 5.85 mmol/l. His BAT SFF (87%, measured both after cold exposure and warm conditions) and T2*time (19.2 ms after cold exposure and 19.7 ms on ambient conditions) were the highest among all volunteers, and actually they were close to SFF (90% and 90%, respectively) and T2* time (20.7 ms and 21.2 ms) of his WAT. We concluded that this subject had no measurable BAT. Curiously, he was also the only one with elevated blood pressure (154/95 mmHg) and blood cholesterol levels (total cholesterol 7.4 mmol/l, HDL-cholesterol 1.5 mmol/l, LDL-cholesterol 5.2 mmol/l and triglycerides 1.4 mmol/l).

Table 1 – Characteristics of the study participants and the correlation to BAT glucose uptake during cold exposure.

Characteristic (unit)	Mean	Correlation to BAT glucose uptake	
		p value	*r* value
Age (years)	32.7 ± 9.9	0.30	−0.31
Weight (kg)	72.5 ± 10	0.65	0.16
BMI (kg/m^2)	24.4 ± 3.1	0.74	0.11
Waist (cm)	84.6 ± 9.5	0.84	−0.07
Hip (cm)	100.9 ± 7.3	0.70	0.14
BAT SFF during cold exposure (%)	**81.9 ± 4.0**	**0.02**	**−0.64**
BAT SFF at ambient temperature (%)	**82.3 ± 3.8**	**0.02**	**−0.63**
WAT SFF during cold exposure (%)	90.0 ± 2.9	0.84	0.06
WAT SFF at ambient temperature (%)	89.1 ± 3.2	0.75	0.10
Muscle SFF during cold exposure (%)	6.7 ± 1.4	0.33	−0.29
Muscle SFF at ambient temperature (%)	7.6 ± 2.4	0.55	−0.18
BAT T2* relaxation time during cold exposure (ms)	**15.3 ± 1.1**	**0.001**	**−0.79**
BAT T2* relaxation time at ambient temperature (ms)	**14.8 ± 1.8**	**0.02**	**−0.65**
WAT T2* relaxation time during cold exposure (ms)	20.7 ± 2.0	0.52	0.20
WAT T2* relaxation time at ambient temperature (ms)	20.4 ± 1.4	0.38	0.26
Muscle T2* relaxation time during cold exposure (ms)	28.6 ± 3.4	0.70	−0.12
Muscle T2* relaxation time at ambient temperature (ms)	25.6 ± 3.4	0.98	−0.01

4. Discussion

4.1. *Interpretation*

We validated SFF and T2* relaxation time mapping measurements of the supraclavicular fat depot in vivo at 3 T, during both cold exposure and at ambient temperature, and results were compared to ^{18}F-FDG PET measurements obtained during cold exposure. To the best of our knowledge, there are no previous PET–MRI studies which have compared MR properties and ^{18}F-FDG-PET in the same session, using a 3 T PET–MRI scanner. Our results suggested markedly higher water content (and lower fat triglyceride content) in supraclavicular fat as compared to subcutaneous fat WAT. The values on BAT, WAT and muscle differed significantly from each other on SFF maps, T2* maps and ^{18}F-FDG PET, as were expected. SFF maps have superior anatomical quality and resolution compared to T2*map or PET images, and indeed it seems that areas corresponding to lower triglyceride content could be assessed visually. Our results suggest that both SFF and T2* maps are robust parameters for measuring BAT, indicating that MR imaging alone could be used for identification and quantification of BAT.

Table 2 – SFF, T2* time and PET ^{18}F-FDG uptake of BAT, WAT and muscle.

Tissue	SFF	T2*	^{18}F-FDG PET
	%	ms	μmol/100 g/min
BAT (during cold exposure)	81.9 ± 4.0	15.3 ± 1.1	14.4 ± 8.7
BAT(in ambient conditions)	82.3 ± 3.8	14.8 ± 1.8	
WAT (during cold exposure)	90.0 ± 2.9	20.7 ± 2.0	3.0 ± 1.2
WAT (in ambient conditions)	89.1 ± 3.2	20.4 ± 1.4	
muscle (during cold exposure)	6.7 ± 1.4	28.6 ± 3.4	2.7 ± 0.7
muscle (in ambient conditions)	7.6 ± 2.4	25.6 ± 3.4	

Previously, BAT has been detected in humans by ^{18}F-FDG PET, which requires metabolic activation through cold exposure. This is an uncomfortable and lengthy procedure. MRI availability is better compared to PET imaging, and it involves no radiation exposure. Because of the gradual transition from "classical" BAT to beige or "brite" fat and finally subcutaneous WAT, there is a need for methods to estimate the water and triglyceride content and the anatomy of fat tissue. MR-based sequences such as SFF mapping and T2* mapping seem to be best suited for this purpose. Both MR imaging and ^{18}F-FDG-PET have been used to investigate BAT and its association with obesity and insulin resistance.

According to our study, it seems that SFF mapping and T2* mapping can assess BAT independent of cold activation. It has been previously proposed that SFF in BAT would be lower during cold exposure [21,22], due to increased perfusion and thus amount of water in the tissue, and consumption of triglycerides in activated BAT. In a previous study, where SFF was measured repeatedly with the temporal resolution of 5 min over a total measurement time of 140 min, SFF was found to decrease in BAT during cold exposure [22]. However, their VOIs on assumed most activated BAT were small, the mean volume being 1.31 ml, compared to our VOIs which were segmented to contain whole of the supraclavicular fat depot and were about 20-fold in volume compared to theirs. BAT contains a mixture of brown and white adipocytes, and we wanted to take into account the whole volume, not only the strongest activation. Larger VOIs have also been previously used in the literature [21]. It is possible that with larger volume containing both BAT and WAT, the small changes in SFF were not significant because of the averaging effect, and with a larger and more heterogeneous group of subjects there might have been a significant difference. The supraclavicular area is well vascularized [11,27], and previously it has been shown that the changes in SFF during cold exposure probably result from both increased perfusion and lipid consumption [21]. We meticulously excluded the vascular structures while segmenting the fat, so in our study the perfusion effect should be minimized.

Volumes of interest included the whole anatomical supraclavicular fat depot. With our method, we could easily have measured the volume of any given range of SFF or T2* time values. During the time we were planning the layout of the study, there were no set cutoff points in the literature for SFF and T2* values for BAT, and since the results were significant even while we were using the volume of the whole supraclavicular fat deposit, we thought measuring the whole area would be more prudent.

According to our findings, T2* relaxation times of BAT and WAT were slightly higher during cold exposure, but the change was not significant. The T2* values at ambient conditions were in line with previous findings [20,28], when taking into account the age of the subjects. SFF values were overall slightly higher than in previous studies [17,28], but the differences in SFF values measured in BAT and WAT were comparable to previous findings when subject age is taken into account (some of the subjects in other studies were infants). In our study, there was no correlation of BAT ^{18}F-FDG uptake, SFF or T2* values with age or BMI. The reason might be that there was little variation in the weight and the age of the subjects. With a more heterogenous group there might have been a significant correlation.

4.2. *Perspective*

BAT functionality has been assessed previously via fMRI BOLD signal changes [16] and dynamic T2* imaging [17] during cold stimulation, revealing signal fluctuation, but also large heterogeneity in time signature. In one study, SFF was measured at baseline, after cold exposure and after subsequent short reheating, SFF values decreased slightly [21]. The subjects were not imaged with ^{18}F-FDG PET. A second study, involving five subjects, assessed the volume and function of BAT using SFF mapping at ambient temperature and functional BOLD MR imaging during cold exposure observing a correlation with ^{18}F-FDG-PET/CT [16], and another study showed fat fraction (triglyceride content) differences between lean and obese children and infants [20]. However, in the latter study results were not correlated with glucose uptake measured by ^{18}F-FDG-PET because of the limitations for using PET in children. A recent study assessed SFF on oncologic pediatric patients with a control group of geriatric patients, demonstrating that SFF analysis is a reproducible imaging modality for the detection of human BAT and suggesting that SFF might be more reliable parameter for BAT than the commonly used PET signal [19]. Interestingly, in contrast to our results, the SFF values of BAT in that study were independent from its metabolic activity measured by ^{18}F-FDG-PET; this may be due to lack of cold exposure in that study, preventing maximal metabolic activation of BAT.

4.3. *Implications*

Our results suggest that MR imaging methods can, independent of BAT activation, identify supraclavicular fat depot T2* time and SFF, indirect measures of triglyceride content. Thus it is possible to avoid uncomfortable and inconvenient cold exposure and radiation exposure related to ^{18}F-FDG-PET experiments. Further studies are needed to gain more insight into the role of MRI to determine BAT properties and to study the significance of BAT in human physiology and pathophysiology.

Author Contributions

M.H. wrote the manuscript, participated in the experimental design, conducted imaging and analyzed MRI data. M.P. and K.K. participated in the experimental design, conducted imaging and drafted the manuscript. T.S. conducted imaging, analyzed PET data and reviewed and edited the manuscript. J.R. examined the patients clinically, analyzed the metabolic and anthropometric data and edited the manuscript. R.J.H.B. participated in the experimental design, conducted imaging and reviewed and edited the manuscript. P.N. and R.P. participated in the study design and reviewed and edited the manuscript. K.A.V. participated in the study design, conducted imaging and reviewed and edited the manuscript.

All of the authors approved the final version of the manuscript.

Funding

The study was conducted within the Finnish Centre of Excellence in Cardiovascular and Metabolic Diseases supported by the Academy of Finland, University of Turku, Turku University Hospital and Åbo Akademi University. All experiments were performed in the Turku PET Centre, University of Turku and Turku University Hospital, Turku, Finland. This study has also received funding by the European Union as well as personal grants from Turku University Hospital (M.H., R.P., V.S., K.K.), the Academy of Finland (K.A.V., R.J.H.B.), the National Graduate School of Clinical Investigation (M.H.), Southwestern Finland Cultural Foundation (K.A. V) and the Paulo Foundation (K.A.V., R.J.H.B.).

Disclosure Statement

No potential conflict of interest relevant to this article is reported by the authors.

Acknowledgments

We thank the staff of Turku PET Centre for their outstanding technical assistance.

REFERENCES

[1] Cinti S. The adipose organ at a glance. Dis Model Mech 2012;5:588–94.
[2] Lee P, Greenfield JR, Ho KK, Fulham MJ. A critical appraisal of the prevalence and metabolic significance of brown adipose tissue in adult humans. Am J Physiol Endocrinol Metab 2010;299:E601–6.
[3] Saito M, Okamatsu-Ogura Y, Matsushita M, et al. High incidence of metabolically active brown adipose tissue in healthy adult humans: effects of cold exposure and adiposity. Diabetes 2009;58:1526–31.

[4] Drubach LA, Palmer III EL, Connolly LP, Baker A, Zurakowski D, Cypess AM. Pediatric brown adipose tissue: detection, epidemiology, and differences from adults. J Pediatr 2011;159: 939–44.
[5] Yoneshiro T, Aita S, Matsushita M, et al. Age-related decrease in cold-activated brown adipose tissue and accumulation of body fat in healthy humans. Obesity (Silver Spring) 2011;19:1755–60.
[6] Lidell ME, Betz MJ, Dahlqvist LO, et al. Evidence for two types of brown adipose tissue in humans. Nat Med 2013;19:631–4.
[7] Wu J, Bostrom P, Sparks LM, et al. Beige adipocytes are a distinct type of thermogenic fat cell in mouse and human. Cell 2012;150:366–76.
[8] Rosenwald M, Perdikari A, Rulicke T, Wolfrum C. Bi-directional interconversion of brite and white adipocytes. Nat Cell Biol 2013;15:659–67.
[9] van Marken Lichtenbelt WD, Vanhommerig JW, Smulders NM, et al. Cold-activated brown adipose tissue in healthy men. N Engl J Med 2009;360:1500–8.
[10] Virtanen KA, Lidell ME, Orava J, et al. Functional brown adipose tissue in healthy adults. N Engl J Med 2009;360:1518–25.
[11] Orava J, Nuutila P, Lidell ME, et al. Different metabolic responses of human brown adipose tissue to activation by cold and insulin. Cell Metab 2011;14:272–9.
[12] Orava J, Nuutila P, Noponen T, et al. Blunted metabolic responses to cold and insulin stimulation in brown adipose tissue of obese humans. Obesity (Silver Spring) 2013;11:2279–87.
[13] Cypess AM, Lehman S, Williams G, et al. Identification and importance of brown adipose tissue in adult humans. N Engl J Med 2009;360:1509–17.
[14] Yoneshiro T, Aita S, Matsushita M, et al. Brown adipose tissue, whole-body energy expenditure, and thermogenesis in healthy adult men. Obesity (Silver Spring) 2011;19:13–6.
[15] Hamilton G, Smith Jr DL, Bydder M, Nayak KS, Hu HH. MR properties of brown and white adipose tissues. J Magn Reson Imaging 2011;34:468–73.
[16] Chen YC, Cypess AM, Chen YC, et al. Measurement of human brown adipose tissue volume and activity using anatomic MR imaging and functional MR imaging. J Nucl Med 2013;54:1584–7.
[17] van Rooijen BD, van der Lans AA, Brans B, et al. Imaging cold-activated brown adipose tissue using dynamic T2*-weighted magnetic resonance imaging and 2-deoxy-2-[18F]fluoro-D-glucose positron emission tomography. Invest Radiol 2013;48: 708–14.
[18] Deng J, Schoeneman SE, Zhang H, et al. MRI characterization of brown adipose tissue in obese and normal-weight children. Pediatr Radiol 2015;45:1682–9.
[19] Franz D, Karampinos DC, Rummeny EJ, et al. Discrimination between brown and white adipose tissue using a 2-point Dixon water–fat separation method in simultaneous PET/MRI. J Nucl Med 2015;56:1742–7.
[20] Hu HH, Yin L, Aggabao PC, Perkins TG, Chia JM, Gilsanz V. Comparison of brown and white adipose tissues in infants and children with chemical-shift-encoded water-fat MRI. J Magn Reson Imaging 2013;38:885–96.
[21] Lundstrom E, Strand R, Johansson L, Bergsten P, Ahlstrom H, Kullberg J. Magnetic resonance imaging cooling-reheating protocol indicates decreased fat fraction via lipid consumption in suspected brown adipose tissue. PLoS One 2015;10:e0126705.
[22] Stahl V, Maier F, Freitag MT, et al. In vivo assessment of cold stimulation effects on the fat fraction of brown adipose tissue using DIXON MRI. J Magn Reson Imaging 2016.
[23] Raiko J, Holstila M, Virtanen KA, et al. Brown adipose tissue triglyceride content is associated with decreased insulin sensitivity, independently of age and obesity. Diabetes Obes Metab 2015;17:516–9.
[24] Dixon WT. Simple proton spectroscopic imaging. Radiology 1984;153:189–94.
[25] Eggers H, Brendel B, Duijndam A, Herigault G. Dual-echo Dixon imaging with flexible choice of echo times. Magn Reson Med 2011;65:96–107.
[26] Chavhan GB, Babyn PS, Thomas B, Shroff MM, Haacke EM. Principles, techniques, and applications of T2*-based MR imaging and its special applications. Radiographics 2009;29: 1433–49.
[27] Din U, Raiko J, Saari T, et al. Human brown adipose tissue [(15)O]O2 PET imaging in the presence and absence of cold stimulus. Eur J Nucl Med Mol Imaging 2016;43: 1878–86.
[28] Hu HH, Perkins TG, Chia JM, Gilsanz V. Characterization of human brown adipose tissue by chemical-shift water-fat MRI. AJR Am J Roentgenol 2013;200:177–83.